Journal of
Synchrotron
Radiation

ISSN 0909-0495

Received 3 May 2010
Accepted 30 July 2010

Time-resolved SAXS measurements facilitated by online HPLC buffer exchange

Malene Hillerup Jensen,[a,b]* Katrine Nørgaard Toft,[a] Gabriel David,[c] Svend Havelund,[b] Javier Pérez[c]* and Bente Vestergaard[a]

[a]Department of Medicinal Chemistry, Faculty of Pharmaceutical Sciences, University of Copenhagen, Denmark, [b]Novo Nordisk A/S, Denmark, and [c]Synchrotron Soleil, L'Orme des Merisiers, Saint-Aubin, BP 48, 91192 Gif-sur-Yvette, France. E-mail: mhij@farma.ku.dk, javier.perez@synchrotron-soleil.fr

Small-angle X-ray scattering (SAXS) is a powerful technique to structurally characterize biological macromolecules in solution. Heterogeneous solutions are inherently challenging to study. However, since SAXS data from ideal solutions are additive, with careful computational analysis it may be possible to separate contributions from individual species present in solution. Hence, time-resolved SAXS (TR-SAXS) data of processes in development can be analyzed. Many reported TR-SAXS results are initialized by a sudden change in buffer conditions facilitated by rapid mixing combined with either continuous or stopped flow. In this paper a method for obtaining TR-SAXS data from systems where the reaction is triggered by removal of a species is presented. This method is based on fast buffer exchange over a short desalting column facilitated by an online HPLC (high-performance liquid chromatography) connected to the SAXS sample cell. The sample is stopped in the sample cell and the evolving reaction is followed. In this specific system the removal of phenol initiates a self-association process of long-acting insulin analogues. For this experiment, data were collected in time series while varying concentrations. The method can be generally applied to other systems where removal of a species or other changes in experimental conditions trigger a process.

© 2010 International Union of Crystallography
Printed in Singapore – all rights reserved

Keywords: time-resolved small-angle X-ray scattering; TR-SAXS; SAXS; HPLC; HPLC-SAXS; long-acting insulin analogue.

1. Introduction

Time-resolved small-angle X-ray scattering (TR-SAXS) experiments have been carried out for decades and have provided valuable structural insight into mechanisms within various fields. Protein and RNA folding (Kwok *et al.*, 2006; Lamb *et al.*, 2008; Russell *et al.*, 2000; Segel *et al.*, 1999; Semisotnov *et al.*, 1996), structural changes in vira (Lee *et al.*, 2004; Pérez *et al.*, 2000), changes in quaternary structures owing to enzymatic reactions (Tsuruta *et al.*, 2005), fibrillation (Oliveira *et al.*, 2009; Vestergaard *et al.*, 2007), self-assembly of silica-film (Grosso *et al.*, 2002), micelles (Schmolzer *et al.*, 2002) and nanoparticles (Tobler *et al.*, 2009) are examples hereof. We are interested in studying self-association of human insulin analogues.

Obtaining good TR-SAXS data is highly dependent on the triggering mechanism of the system and the timescale of the experiment under scrutiny. The time span of a reaction can range from picoseconds to hours and days. Naturally, the fast processes are especially challenging to investigate. In all cases it is evident that the starting point of the reaction and the SAXS measurements must be closely coordinated, in order to capture the full process. Triggering of a process can be achieved differently. Reported mechanisms are sample dilution (Pollack *et al.*, 1999; Segel *et al.*, 1999), change in temperature (Grigoriew *et al.*, 2001), pressure (Raudino *et al.*, 2004*a*,*b*), pH (Akiyama *et al.*, 2002; Uzawa *et al.*, 2004, 2006) or, for example, laser illumination (Cammarata *et al.*, 2008, 2009), which commences the process.

Special devices designed to mix two liquids together (sample and trigger component) have been reported earlier (Marmiroli *et al.*, 2009; Pollack *et al.*, 1999; Tsuruta *et al.*, 1989). The stopped-flow and continuous-flow techniques in a microfluidic chip also containing a SAXS sample chamber enable fast mixing times followed by short exposures in the range of nanoseconds to milliseconds. At present, arguably the most sophisticated method for ultrafast time-resolved wide-angle X-ray scattering (TR-WAXS) with nanosecond time resolution is facilitated by coordinated delayed X-ray and laser pulses. Transient structures are generated by timed laser pulses; subsequently data of each particular transient structure are detected by means of a chopper system, which assures that

only scattering from specific time points are collected by the detector. This method also circumvents the problem of erasing the detector between the very short exposures (Andersson *et al.*, 2009; Cammarata *et al.*, 2008, 2009).

These techniques have proven very effective for reactions which are initiated by addition of a compound. However, when a reaction is dependent on the removal of a component, the only reported method is dilution of the sample to obtain a lower effective concentration of the component, as is seen with, for example, guanidinium chloride and urea for refolding studies (Pollack *et al.*, 1999; Segel *et al.*, 1999). However, the disadvantage is that the system under investigation is equally diluted, and very dilute samples are not attractive for SAXS measurements, where the data quality often suffers. Secondly, the protein concentration may influence the structural state of the system investigated.

In the system we wish to investigate here, *i.e.* the self-association of long-acting insulin analogues, the trigger mechanism is the removal of phenol from the sample environment (Jonassen *et al.*, 2006) (see Fig. 1). These types of insulin analogues have been designed to, upon subcutaneous injection, form a depot of aggregates for slow release into the interstitial fluid. The protracted action is facilitated by acylation, where fatty acid or bile acid side-chains are linked to Lys^{B29} in the B-chain of insulin (Havelund *et al.*, 2004; Jonassen *et al.*, 2006). Phenol and phenolic derivatives (m-cresol) are present in the pharmacological preparation used as preservatives; however, they furthermore bind in the interface between dimers in the insulin hexamers (see Fig. 1). Removal of phenol causes a structural change between the R_6 and T_6 state of the insulin hexamer. The conformational change induced is believed to trigger self-association of the insulin analogues (see Fig. 1).

SAXS studies of the developing self-association would provide invaluable structural insight to the mechanism and hence both an understanding of the existing analogues and structural basis for further development.

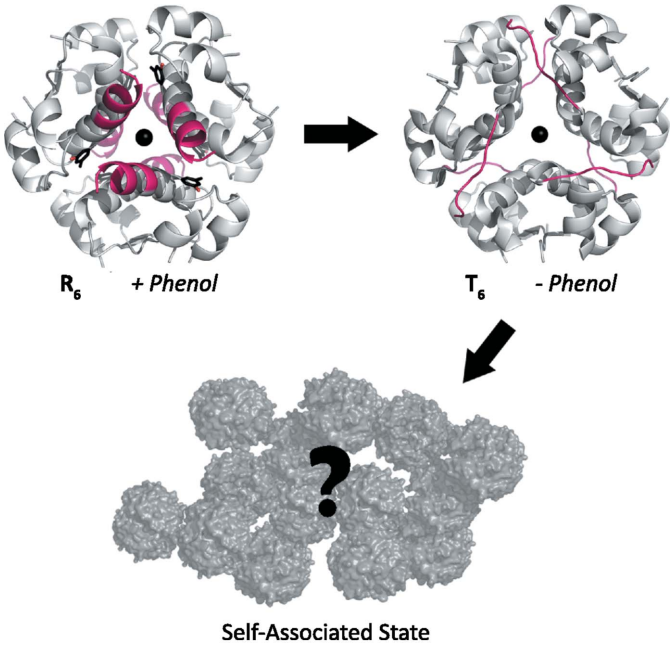

Figure 1
Triggering mechanism: self-association of acylated insulin analogues begins from the T_6 state upon removal of phenol. In the presence and absence of phenol the insulin hexamer exists in the relaxed (R_6) and the tense state (T_6), respectively. The major change happens in the N-terminal of the B-chain (red), which adopts different conformations in the two states. Zinc ions (black) coordinate insulin monomers in the central axis of the hexamer. The human insulin analogue is acylated at Lys^{B29}. Lys^{B29} and the acylations (side chains) are not shown in this figure.

2. Experimental set-up

2.1. Sample preparation

The insulin analogue Lys^{B29} ($N^{\varepsilon}\omega$-carboxyheptadecanoyl) desB30 human insulin (ωchl) was solubilized in a buffered solution containing 10 m*M* Tris-HCl pH 7.4 and 32 m*M* phenol. The protein concentration was 2.4 m*M* and Zn^{2+} ions were present in a concentration of six Zn^{2+} ions per six insulin molecules. This composition is similar to the pharmacologically relevant preparation with respect to phenol, and zinc ion concentration. The zinc ions are present to ensure formation of hexamers of the insulin analogues in the solution.

2.2. Fast buffer exchange by high-performance liquid chromatography (HPLC)

At the SWING beamline at Synchrotron Soleil, the SAXS sample chamber is connected online to an HPLC (Agilent 1200 series) (David & Pérez, 2009). This facilitates separation of molecules immediately before collection of SAXS data. The principle of the time-resolved SAXS data collection in this manuscript is quick buffer exchange *via* a short desalting

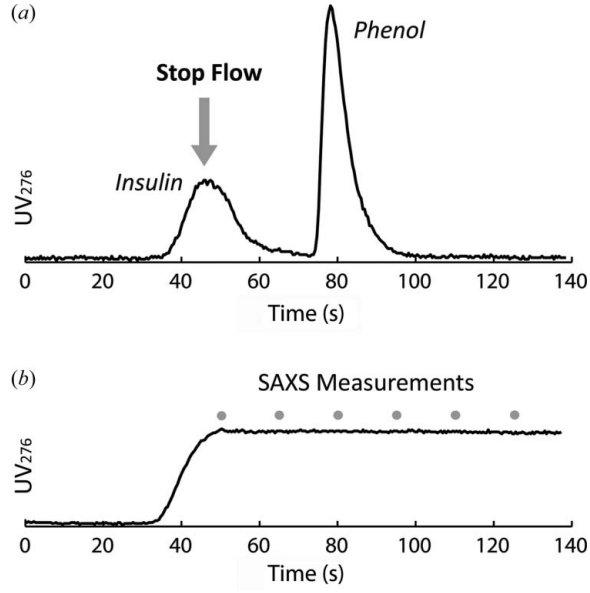

Figure 2
Schematic representation of the principle used in halted flow. (*a*) The UV signal from the SAXS sample cell, where insulin is separated from phenol. (*b*) The UV signal during halted flow. The UV signal is constant while the protein sample is static in the SAXS cell, and SAXS data are collected (grey dots).

column prior to SAXS measurements. Insulin elutes before phenol, as can be seen in Fig. 2(*a*). The sample (*i.e.* the insulin peak) enters the SAXS sample cell and the flow is stopped at maximum concentration followed by X-ray exposure over predefined time ranges (Fig. 2*b*). The UV signal was monitored both on the HPLC and directly in the SAXS sample chamber. The UV signal from the solution in the SAXS sample chamber is essential for timing of the experiment.

The HPLC has capillaries with an inner diameter of 250 µm; however, the sample cell is composed of a quartz capillary with an inner diameter of 1.6 mm (David & Pérez, 2009). This means that part of the resolution between the two chromatographic peaks is lost upon entry in the sample cell. Therefore a suitable desalting column is crucial to ensure proper separation of the two peaks. A BioSuite HR column (5 µm, 6 × 40 mm, pore size 125 Å) was chosen for the experiment. The retention time of insulin was 50 s at a flow of 1 ml min^{-1} with an elution buffer consisting of 10 m*M* Tris-HCl pH 7.4, 140 m*M* NaCl, 0.6 m*M* phenol and 0.01% NaN_3 at 298 K. A small amount of phenol was added to the eluent in order to slow down the rate of self-association of insulin analogue ωchl.

2.3. Halted flow

In order to stop the flow during data acquisition, a valve was installed (David & Pérez, 2009) between the HPLC and the SAXS sample chamber (see Fig. 3). The insulin peak passes the open valve and subsequently when it enters the SAXS sample chamber the valve was switched (Fig. 3*a*). The flow after the valve was stopped, while the flow of buffer/sample before the valve went into waste (Fig. 3*b*). With the correct timing of the valve, the sample is paused in the sample chamber in position for X-ray exposure. The UV signal of the static protein sample in the SAXS sample chamber is shown in Fig. 2(*b*). The timing from injection to the correct time point for switching the valve was optimized by successive trials. The timing depends on the injection volume, the flow rate and the time range of interest during data acquisition.

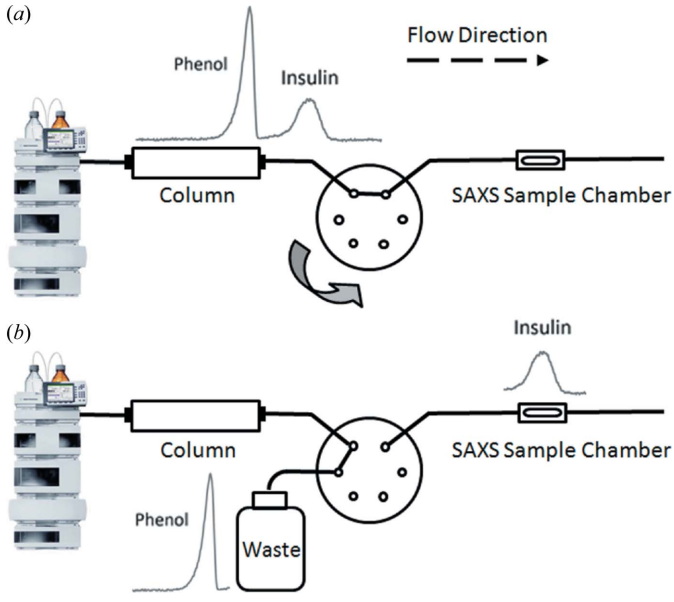

Figure 3
Scheme representing the experimental set-up. A valve is installed between the desalting column and the SAXS sample chamber. When the maximum of the insulin peak passes through the SAXS sample cell, the flow is stopped by switching of the valve (*a*). Thereby the insulin sample is stopped in the sample chamber, while the phenol runs directly to the waste (*b*).

2.4. TR-SAXS data collection

SAXS data were collected at the SWING beamline at Synchrotron Soleil, Paris. The intensity as a function of the magnitude of the scattering vector [$q = 4\pi\sin(\theta)/\lambda$, where 2θ equals the scattering angle] was collected in the q-range $0.0054 < q < 0.59$ Å^{-1} with an X-ray wavelength of $\lambda = 1.05$ Å. The scattering was collected on a AVIEX170170 CCD detector in vacuum.

Data were collected in time series in the range 0–6 min and in concentration series. Injection volumes of 25–100 µl were used to obtain different protein concentrations for the SAXS experiment. The data collection of the time series (50 µl) was repeated three times in order to estimate the reproducibility of the experiment. Preceding experiments using time-resolved dynamic light scattering (TR-DLS) suggested which time ranges to investigate. The exposure time was 1 or 4 s, and 20 frames were collected within each time range. Buffer measurements were performed immediately prior to the protein measurements (20 frames were collected and averaged).

2.5. Data processing and analysis

Radial averaging was performed using the program *ActionJava* locally developed at the SWING beamline. The data were normalized with respect to the transmitted beam. Scaling of the data was achieved using water as a reference. Silver behenate was utilized for q-scaling. Buffer subtraction was carried out as a routine in *MATLAB* enabling handling of large amounts of data.

The lower-concentration data (25 µl) contained a lower signal-to-noise ratio; however, the data still contain valuable information in the lower q-ranges. Data analysis was performed using the *Atsas* package (Konarev *et al.*, 2006). The radius of gyration, R_g, was estimated with the Guinier approximation using the manual Guinier feature in the *Primus* suite (Konarev *et al.*, 2003). Because of the oligomers formed in solution it was difficult to find a good Guinier range; however, a qR_g value of no higher than 1.3 was used to ensure the quality of the estimation (and $qR_g \simeq 1.4$ for the most self-associated samples at high concentration, injection volume 100 µl).

3. Results and discussion

The method described above enabled collection of TR-SAXS data of a self-associating insulin analogue. The developing self-association can be seen in the scattering curves in Fig. 4.

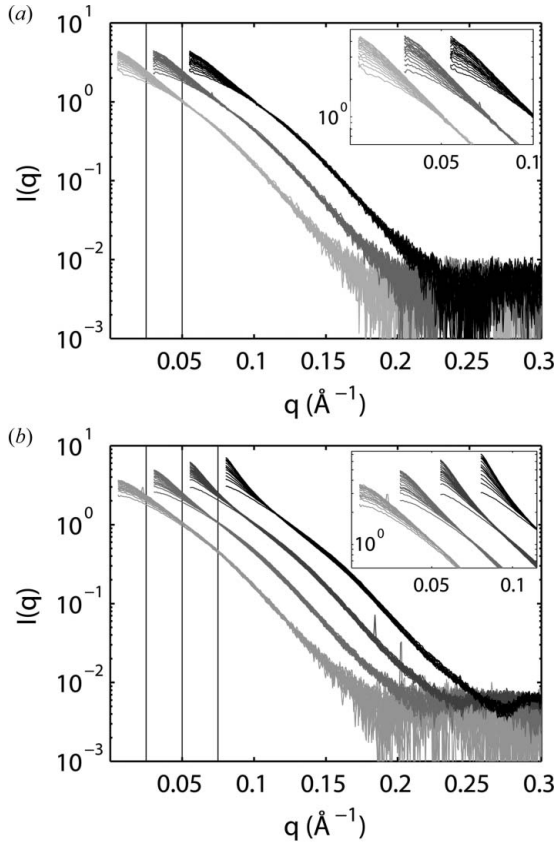

Figure 4
TR-SAXS data of insulin analogue ωchl. (*a*) A triplet of data series collected in the time range 0–6 min (injection volume 50 µl). (*b*) SAXS data collected at four different concentrations (time range 0–6 min) by variation in injection volumes: 25 µl, 50 µl, 75 µl and 100 µl in shades from grey to black. The data series have been shifted along the abscissa for a better view. The grey lines indicate the individual start points ($q = 0$) for the shifted data series. The data series of reproducibility and the concentration series were collected on two different occasions.

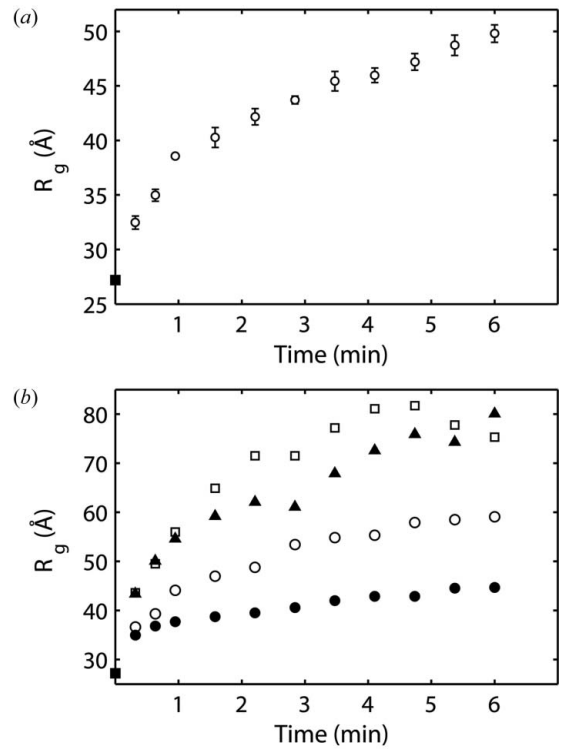

Figure 5
R_g plots from data of the reproducibility series and concentration series. (*a*) The average R_g value (obtained from three identical series) is plotted *versus* time in the time range 0–6 min (empty circles). The standard deviation is indicated with error bars at each data point. R_g is plotted *versus* time (*b*) in the concentration series 25 µl (filled circles), 50 µl (circles), 75 µl (filled triangles) and 100 µl (squares) collected in the time range 0–6 min. The R_g of insulin analogue ωchl prior to self-association (in the dodecameric state) is represented by a black square.

Data of ωchl in the time range (0–6 min) are shown in Fig. 4(*a*). I_0 scales as $MW \times C$, where MW is the apparent molar mass of the average object in solution, and C is the mass concentration, which does not change within the individual data series. The increase in size is clearly seen as an increased intensity at low q-values. A cross-over point among the scattering curves is seen at about 0.05 Å^{-1} as a result of the increasing self-association.

Fig. 4(*a*) shows three series collected to estimate the reproducibility of the experiment. Series 2 and 3 were scaled on the intensity with factors 0.94 and 0.97 with respect to series 1. These slight variations can originate from small concentration differences and the fact that self-association is a stochastic process. The average R_g with standard deviations can be seen in Fig. 5(*a*) which shows reproducibility with a maximum standard deviation of 1 Å. The time range 0–6 min shows a steep increase in R_g ending in a slow increasing plateau at about 50 Å, in comparison with an R_g of 27 Å for an insulin dodecamer (in the presence of 32 m*M* phenol).

The data collected at varying concentrations, applying 25, 50, 75 and 100 µl of sample to the column (Fig. 4*b*), also reveal a clear development at low q-values (time range 0–6 min). It is evident from this experiment that the state of self-association is very dependent on the protein concentration. This is confirmed by TR-DLS measurements (not shown here). Visual inspection of I_0 of the concentration series in Fig. 4(*b*) clearly shows this dependency. The I_0 of the first data curve of the higher concentrations (50, 75 and 100 µl injection volume) are at a level of 2.3, 4.2 and 5.8, respectively, relative to the low concentration (25 µl). The R_g plot (Fig. 5*b*) furthermore illustrates this tendency. The R_g increases as a function of time. The data from injection volumes 25, 50, 75 and 100 µl reach levels of 45, 60, 75 and 80 Å, respectively.

When using a powerful radiation source for investigating dynamic processes it is necessary to take into account the effect that an X-ray beam may have on the system of interest; this can be in relation to radiation damage or radiation induction of the process. An example of the second matter is an X-ray triggered crystallization of self-assembling filament networks of a short peptide (Cui *et al.*, 2010). To address this issue, we have used two methods to evaluate whether X-ray radiation has an effect on self-association: (i) collection and comparison of consecutive and overlapping time series and (ii) X-ray exposure of the self-associating sample followed by NUV-CD where the conversion from R_6 to the T_6 state of the

hexamers can be followed. The latter example is specific to the system investigated here.

4. Conclusion

Here, a method for collecting TR-SAXS data for a system triggered by a buffer exchange or removal of a buffer component is presented. The suitability of this technique is dependent on the rate of the reaction studied. The reaction rates which can be studied are on the minute timescale, and can be varied to suit the system under investigation. There are several advantages of this method. The sample consumption is low compared with continuous-flow SAXS measurements. Furthermore, the demands for equipment are very modest, and no advanced chip development is needed. In addition, heterogeneous triggering is not a concern, since the entire sample experiences the same buffer environment. In particular, a large advantage is that this method enables studying of processes without significant dilution of the sample. An example of an application which could benefit from this technique is, for example, when studying systems where different oligomeric states of a protein exist in equilibrium. In the case of calreticulin, a chaperone of the endoplasmic reticulum, an equilibrium exists between monomers and dimers in solution (Nørgaard *et al.*, 2008). Using the approach presented here, separation of the two species is possible, thus yielding data on pure monodisperse samples, and a re-establishment of the equilibrium can be followed by varying the speed or column type, thus yielding valuable information about the timescale and nature of the protein–protein interactions. In summary, this paper illustrates an alternative approach to TR-SAXS measurements.

References

Akiyama, S., Takahashi, S., Kimura, T., Ishimori, K., Morishima, I., Nishikawa, Y. & Fujisawa, T. (2002). *Proc. Natl Acad. Sci. USA*, **99**, 1329–1334.

Andersson, M., Malmerberg, E., Westenhoff, S., Katona, G., Cammarata, M., Wohri, A. B., Johansson, L. C., Ewald, F., Eklund, M., Wulff, M., Davidsson, J. & Neutze, R. (2009). *Structure*, **17**, 1265–1275.

Cammarata, M., Eybert, L., Ewald, F., Reichenbach, W., Wulff, M., Anfinrud, P., Schotte, F., Plech, A., Kong, Q., Lorenc, M., Lindenau, B., Rabiger, J. & Polachowski, S. (2009). *Rev. Sci. Instrum.* **80**, 015101.

Cammarata, M., Levantino, M., Schotte, F., Anfinrud, P. A., Ewald, F., Choi, J., Cupane, A., Wulff, M. & Ihee, H. (2008). *Nat. Methods*, **5**, 881–886.

Cui, H., Pashuck, E. T., Velichko, Y. S., Weigand, S. J., Cheetham, A. G., Newcomb, C. J. & Stupp, S. I. (2010). *Science*, **327**, 555–559.

David, G. & Pérez, J. (2009). *J. Appl. Cryst.* **42**, 892–900.

Grigoriew, H., Chmielewski, A. G. & Amenitsch, H. (2001). *Polymer*, **42**, 103–108.

Grosso, D., Babonneau, F., Albouy, P. A., Amenitsch, H., Balkenende, A. R., Brunet-Bruneau, A. & Rivory, J. (2002). *Chem. Mater.* **14**, 931–939.

Havelund, S., Plum, A., Ribel, U., Jonassen, I., Volund, A., Markussen, J. & Kurtzhals, P. (2004). *Pharm. Res.* **21**, 1498–1504.

Jonassen, I., Havelund, S., Ribel, U., Plum, A., Loftager, M., Hoeg-Jensen, T., Volund, A. & Markussen, J. (2006). *Pharm. Res.* **23**, 49–55.

Konarev, P. V., Petoukhov, M. V., Volkov, V. V. & Svergun, D. I. (2006). *J. Appl. Cryst.* **39**, 277–286.

Konarev, P. V., Volkov, V. V., Sokolova, A. V., Koch, M. H. J. & Svergun, D. I. (2003). *J. Appl. Cryst.* **36**, 1277–1282.

Kwok, L. W., Shcherbakova, I., Lamb, J. S., Park, H. Y., Andresen, K., Smith, H., Brenowitz, M. & Pollack, L. (2006). *J. Mol. Biol.* **355**, 282–293.

Lamb, J., Kwok, L., Qiu, X., Andresen, K., Park, H. Y. & Pollack, L. (2008). *J. Appl. Cryst.* **41**, 1046–1052.

Lee, K. K., Gan, L., Tsuruta, H., Hendrix, R. W., Duda, R. L. & Johnson, J. E. (2004). *J. Mol. Biol.* **340**, 419–433.

Marmiroli, B., Grenci, G., Cacho-Nerin, F., Sartori, B., Ferrari, E., Laggner, P., Businaro, L. & Amenitsch, H. (2009). *Lab Chip*, **9**, 2063–2069.

Nørgaard, T. K., Larsen, N., Steen, J. F., Hojrup, P., Houen, G. & Vestergaard, B. (2008). *Biochim. Biophys. Acta*, **1784**, 1265–1270.

Oliveira, C. L. P., Behrens, M. A., Pedersen, J. S., Erlacher, K., Otzen, D. & Pedersen, J. S. (2009). *J. Mol. Biol.* **387**, 147–161.

Pérez, J., Defrenne, S., Witz, J. & Vachette, P. (2000). *Cell. Mol. Biol.* **46**, 937–948.

Pollack, L., Tate, M. W., Darnton, N. C., Knight, J. B., Gruner, S. M., Eaton, W. A. & Austin, R. H. (1999). *Proc. Natl. Acad. Sci. USA*, **96**, 10115–10117.

Raudino, A., Lo Celso, F., Triolo, A. & Triolo, R. (2004*a*). *J. Chem. Phys.* **120**, 3489–3498.

Raudino, A., Lo Celso, F., Triolo, A. & Triolo, R. (2004*b*). *J. Chem. Phys.* **120**, 3499–3507.

Russell, R., Millett, I. S., Doniach, S. & Herschlag, D. (2000). *Nat. Struct. Biol.* **7**, 367–370.

Schmolzer, S., Grabner, D., Gradzielski, M. & Narayanan, T. (2002). *Phys. Rev. Lett.* **88**, 258301.

Segel, D. J., Bachmann, A., Hofrichter, J., Hodgson, K. O., Doniach, S. & Kiefhaber, T. (1999). *J. Mol. Biol.* **288**, 489–499.

Semisotnov, G. V., Kihara, H., Kotova, N. V., Kimura, K., Amemiya, Y., Wakabayashi, K., Serdyuk, I. N., Timchenko, A. A., Chiba, K., Nikaido, K., Ikura, T. & Kuwajima, K. (1996). *J. Mol. Biol.* **262**, 559–574.

Tobler, D. J., Shaw, S. & Benning, L. G. (2009). *Geochim. Cosmochim. Acta*, **73**, 5377–5393.

Tsuruta, H., Kihara, H., Sano, T., Amemiya, Y. & Vachette, P. (2005). *J. Mol. Biol.* **348**, 195–204.

Tsuruta, H., Nagamura, T., Kimura, K., Igarashi, Y., Kajita, A., Wang, Z. X., Wakabayashi, K., Amemiya, Y. & Kihara, H. (1989). *Rev. Sci. Instrum.* **60**, 2356–2358.

Uzawa, T., Akiyama, S., Kimura, T., Takahashi, S., Ishimori, K., Morishima, I. & Fujisawa, T. (2004). *Proc. Natl Acad. Sci. USA*, **101**, 1171–1176.

Uzawa, T., Kimura, T., Ishimori, K., Morishima, I., Matsui, T., Ikeda-Saito, M., Takahashi, S., Akiyama, S. & Fujisawa, T. (2006). *J. Mol. Biol.* **357**, 997–1008.

Vestergaard, B., Groenning, M., Roessle, M., Kastrup, J. S., van de Weert, M., Flink, J. M., Frokjaer, S., Gajhede, M. & Svergun, D. I. (2007). *PLOS Biol.* **5**, 1089–1097.